Mitigation of cross-beam energy transfer in inertial-confinement-fusion plasmas with enhanced laser bandwidth

J. W. Bates,[1] J. F. Myatt,[2] J. G. Shaw,[3] R. K. Follett,[3] J. L. Weaver,[1] R. H. Lehmberg,[1] and S. P. Obenschain[1]

[1]*Plasma Physics Division, U.S. Naval Research Laboratory, Washington, DC 20375, USA*
[2]*Department of Electrical and Computer Engineering, University of Alberta, Edmonton, Alberta, Canada T6G1H9*
[3]*Laboratory for Laser Energetics, University of Rochester, Rochester, New York 14623, USA*

Cross-beam energy transfer (CBET) is a significant energy-loss mechanism in directly driven inertial-confinement-fusion (ICF) targets. One strategy for mitigating CBET is to increase the bandwidth of the laser light, thereby disrupting the resonant three-wave interactions that underlie this nonlinear scattering process. Here, we report on numerical simulations performed with the wave-based code LPSE that show a significant reduction in CBET for bandwidths of $2-5$ THz (corresponding to a normalized bandwidth of $0.2\%-0.6\%$ at a laser wavelength of 351 nm) under realistic plasma conditions. Such bandwidths are beyond those available with current high-energy lasers used for ICF, but could be achieved using stimulated rotation Raman scattering in diatomic gases like nitrogen.

The interference pattern created by the beating of the electric fields of two intense lasers (with angular frequencies ω_1, ω_2 and wave vectors $\mathbf{k}_1, \mathbf{k}_2$) crossing in a plasma can excite a density perturbation due to the ponderomotive force [1]. A state of resonance is reached when the beat frequency $\omega_1 - \omega_2$ and wave vector $\mathbf{k}_a = \mathbf{k}_1 - \mathbf{k}_2$ of the perturbation satisfy the dispersion relation for an ion-acoustic wave

$$\omega_1 - \omega_2 = \mathbf{k}_a \cdot \mathbf{U} \pm k_a c_s, \tag{1}$$

where $\mathbf{U}$ is the plasma flow velocity, $c_s = [(Z k_B T_e + 3 k_B T_i)/m_i]^{1/2}$ is the ion acoustic speed, Z is the ion charge, k_B is the Boltzmann constant, m_i is the ion mass, and T_e and T_i are the electron and ion temperatures, respectively. At resonance, the induced ion-acoustic wave and the two laser beams become parametrically unstable, resulting in the amplification of the plasma density perturbation and a transfer of energy to the beam with lower frequency in the rest frame of the plasma [2]. Inspection of Eq. (1) shows that resonance can occur for two lasers with the same frequency ($\omega_1 = \omega_2$) provided that the speed of the plasma flow is sufficiently supersonic (i.e., that the product of the Mach number $M = U/c_s$ and the cosine of the angle between $\mathbf{k}_a$ and $\mathbf{U}$ equals plus or minus 1), but in such a case the density perturbation is static in the laboratory frame. It is also apparent that small differences between the laser frequencies can shift the location of resonance in the plasma (for spatially dependent velocity profiles) or modify the energy transfer between beams, as has been done in indirect-drive simulations [3,4] and experiments [5–8] on the National Ignition Facility (NIF).

The phenomenon described above is known as induced Brillouin scattering [9] or more commonly, cross-beam energy transfer (CBET) [10–19], and is considered highly deleterious to direct-drive inertial-confinement-fusion (ICF) schemes because it causes a significant amount of the incident laser energy to be scattered away from the target, or to be absorbed

in a less favorable location. Figure 1 depicts the geometry of crossing laser rays with the most-efficient energy transfer in a direct-drive ICF implosion [20]. In the so-called "backscatter mode" of CBET, a ray from the edge of one laser beam refracts through the plasma corona of the target and crosses an incoming ray from another beam. Energy can be transferred from the incoming ray to the outgoing one if the crossing occurs in a region where Eq. (1) is satisfied. In that case, the incoming ray reaches the most absorptive region of the plasma corona where $n_e \simeq n_c$ with less energy than it would have in the absence of CBET, reducing both the ablation pressure and the implosion symmetry. Here, n_e is the electron number density of the plasma, $n_c = m_e \omega_0^2/(4\pi e^2)$ is the critical density for laser absorption, m_e is the electron mass, ω_0 is the angular frequency of the incident light, and e is the electron charge.

In direct-drive ICF experiments performed on the OMEGA laser facility, CBET is thought to be responsible for as much as a 30% reduction in the overall hydrodynamic efficiency of the implosion [21]; for similar target designs scaled to the laser energy of the NIF, this figure is predicted to increase to nearly 50% [22]. To date, several different mitigation strategies have been proposed, including wavelength detuning [23], the use of "mid-Z" ablators [20], and a reduction of the laser spot size [24] to limit beam crossing during the high-intensity portion of the laser pulse. Recent experiments on OMEGA have demonstrated that this last technique does improve the laser-target coupling, but at the price of increased, low-mode surface asymmetries [20]. This effect can be alleviated by focal zooming when the reduction in spot size is delayed until the pellet implodes [25]. Zooming, however, cannot completely eliminate crossing beams or CBET.

A more promising strategy for reducing CBET in ICF targets is to increase the temporal incoherence of the driver—an approach that is theoretically predicted to help mitigate other varieties of parametric instabilities [26–32]. In experiments performed in the 1970s using high-power microwaves to
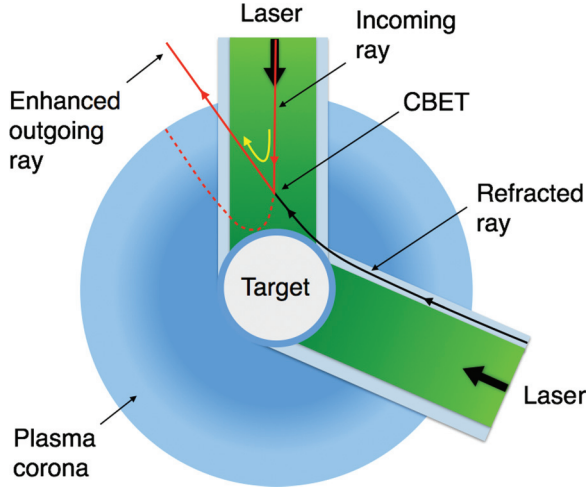
FIG. 1. The backscatter mode of CBET in direct-drive ICF. The yellow arrow denotes the direction of laser energy exchange.

simulate laser-plasma interactions, for example, Obenschain and Luhmann showed that the production of nonthermal electrons from parametric decay was significantly reduced when the bandwidth of the microwaves greatly exceeded the resonance width [33]. More recent theoretical [34–36] and computational [37–39] studies have reached a similar conclusion for the stimulated Brillouin (SBS) and Raman scattering (SRS) of laser light, both of which are important considerations in ICF target designs because they reduce laser-target coupling and in the case of SRS, can generate suprathermal electrons that preheat the thermonuclear fuel, degrading performance. It is generally believed that the mitigation of SBS, SRS, and other laser-plasma instabilities in direct-drive implosions driven by frequency-tripled Nd:glass lasers requires bandwidths of at least several terahertz [40]. Since such values exceed those of most ICF lasers today [41], however, assessing the veracity of this prediction — and in particular, better quantifying the amount of bandwidth necessary to suppress CBET — relies heavily on realistic numerical models for simulating the physics of laser-plasma interactions.

In this Rapid Communication, we present the first numerical simulations demonstrating the efficacy of multiterahertz laser bandwidth for suppressing CBET in direct-drive ICF plasmas. Our simulations were performed with the wave-based code LPSE (laser plasma simulation environment) [42,43] in two-dimensional planar geometry and model the CBET configuration depicted in Fig. 1 in which two laser beams cross at an acute angle in an expanding, supersonic plasma. Using a discrete, multiline bandwidth model, we find a significant reduction in CBET at 2 THz bandwidth (full width at half maximum) and almost complete suppression of CBET at 5 THz. It may be possible to achieve such bandwidths with contemporary ICF lasers by passing beams through gas cells and relying on spectral broadening due to stimulated *rotational* Raman scattering (SRRS), which can occur when a laser excites rotational quantum states of a diatomic molecule [44,45]. This effect has recently been observed in the ultraviolet region on the Nike krypton-fluoride (KrF) laser at the U.S. Naval Research Laboratory (NRL) [46] with only a modest

degradation of the final focal distribution and may provide a practical approach for bandwidth enhancement on other, existing, direct-drive laser facilities [36,40].

Although the CBET phenomenon has been simulated numerically in the past [12,13,15,17], the possibility of using large laser bandwidth as a suppression mechanism for this parametric instability has, to our knowledge, not been investigated previously. Moreover, the LPSE code used in this study contains several significant improvements over previous CBET models that make it particularly well-suited for our purposes here. First, LPSE does not adopt a paraxial approximation (spatial enveloping) or assume transversely periodic boundary conditions, both of which place restrictions on the directions that laser light can propagate and therefore preclude simulations involving complex beam geometries [47–49]. Second, the use of a "total-field–scattered-field" formulation [50–52] in conjunction with a "perfectly matched layer" approach [53] allows laser light to enter and exit through any boundary of the computational domain at arbitrary angles with minimal numerical reflectivity. Third, beams in LPSE simulations can be modeled with realistic laser properties such as speckles, polarization, and bandwidth. Finally, unlike most previous theoretical studies (e.g., Ref. [4]) and ray-based models (e.g., Ref. [20]) of CBET, the LPSE code permits an inhomogeneous background state that can include a time-varying plasma flow. All of these computational features are important for simulating CBET effects accurately in direct-drive ICF plasmas.

The LPSE code solves a system of coupled partial-differential equations governing the evolution of the electric field of the laser $\tilde{\mathbf{E}}$ and the low-frequency plasma response mediated by the ion-acoustic wave. The equations for the electric field are derived by writing $\tilde{\mathbf{E}} = \mathrm{Re}\,[\mathbf{E}(\mathbf{x},t)\exp(-i\omega_0 t)]$ and assuming that the envelope $\mathbf{E}$ varies slowly over the period of the light such that $|\partial^2 \mathbf{E}/\partial t^2| \ll |\omega_0 \partial \mathbf{E}/\partial t|$. This is valid provided that the laser bandwidth $\Delta\nu$ is much less than the central frequency, i.e., $\Delta\nu/\nu_0 \ll 1$, where $\nu_0 = \omega_0/2\pi$ and $\Delta\omega = 2\pi\,\Delta\nu$. (Note that the lasers modeled in the present study have $\nu_0 \gtrsim 850$ THz, so that this inequality is satisfied for bandwidths in the multiterahertz regime.) Then, a combination of Faraday's and Ampère's laws yields

$$\frac{2i\omega_0}{c^2}\frac{\partial}{\partial t}\mathbf{E} + \nabla^2\mathbf{E} - \boldsymbol{\nabla}(\boldsymbol{\nabla}\cdot\mathbf{E}) + \frac{\omega_0^2}{c^2}\varepsilon\mathbf{E} = 0, \qquad (2)$$

where c is the speed of light and we have introduced the plasma dielectric function $\varepsilon = 1 - \omega_{pe}^2/[\omega_0(\omega_0 + i\nu_{ei})]$. Here, $\omega_{pe}^2 = 4\pi e^2 n_e/m_e$ is the square of the plasma frequency, $\nu_{ei} = 4\sqrt{2\pi}Z^2 e^4 n_i \ln\Lambda_e/[3m_e^{1/2}(k_B T_e)^{3/2}]$ is the electron-ion collision frequency (assumed to be small compared to ω_0), $n_i \simeq n_e/Z$ is the ion-number density, and Λ_e is the Coulomb logarithm for electron-ion collisions [1]. The equations that describe the plasma response are derived by decomposing the electron number density and plasma flow velocity as $n_e = n_0 + \delta n$ and $\mathbf{U} = \mathbf{U}_0 + \delta\mathbf{U}$, respectively, where the subscript "0" denotes a static component (assumed to satisfy the plasma hydrodynamic equations to zeroth order) and the symbol δ indicates a small perturbation. We assume that the gradients of static quantities are negligible with respect to those of the perturbations, which is a justified approximation since hydrodynamic length scales ($\gtrsim 100\,\mu$m) in ICF plasmas greatly

exceed the wavelength of an ion-acoustic wave (typically $< 1 \, \mu$m and, in this study, $\simeq 0.2 \, \mu$m). With these assumptions, we find

$$\left(\frac{\partial}{\partial t} + \mathbf{U}_0 \cdot \boldsymbol{\nabla} \right) \frac{\delta n}{n_0} = -w, \qquad (3)$$

$$\left(\frac{\partial}{\partial t} + \mathbf{U}_0 \cdot \boldsymbol{\nabla} + \nu_L \right) w = -\nabla^2 \left(c_s^2 \frac{\delta n}{n_0} + \phi_p \right), \qquad (4)$$

where $w = \boldsymbol{\nabla} \cdot \delta \mathbf{U}$, $\phi_p = Ze^2 |\mathbf{E}|^2 / (4 \, m_e m_i \omega_0^2)$, and ν_L is a nonlocal operator that models the Landau damping of ion-acoustic waves [14,54]. Note that ν_L is applied in k space via a discrete Fourier transform and preserves the linearity of δn over time. More details of the numerical methodology underlying the LPSE code can be found elsewhere [42,43].

We now present results from two-dimensional numerical simulations of CBET that were performed with the LPSE code. We begin our discussion by considering the interaction of two, equal-intensity, monochromatic ($\Delta \nu = 0$) beams crossing at $45°$ in a flowing, inhomogeneous CH plasma (modeled as a single ion species with average charge $Z = 3.5$) near a region of ion-acoustic-wave resonance—an arrangement that approximates the typical backscatter mode of CBET occurring in direct-drive ICF and serves as an archetypal configuration for studying finite-bandwidth effects. The background plasma through which the lasers propagate is $100 \, \mu$m $\times \, 200 \, \mu$m in spatial extent (discretized on a grid with 2000×4000 zones) and is characterized by electron and ion temperatures of 3 and 1 keV, respectively. The plasma is also expanding, with an electron number density n_0 that decreases linearly in the upward direction from $0.4 \, n_c$ to $0.15 \, n_c$. This corresponds to a density gradient scale length $L_n = n_0 / |\boldsymbol{\nabla} n_0| \simeq 200 \, \mu$m, which is representative of values in OMEGA experiments [42]. Additionally, the simulations contain an upwardly directed plasma flow $\mathbf{U}_0$ that varies linearly in space and allows the resonance condition in Eq. (1) to be satisfied. Note that in our simulations, collisional absorption is turned off and ion-acoustic waves are subject to electron Landau damping at a constant rate of $\nu_a = 0.14 \, k_a c_s$, which is a reasonable approximation for the collisionless damping of ion-acoustic waves in a CH plasma under these conditions [55]. Also note that M and n_0 conserve the plasma flux across the computational domain.

Figure 2(a) shows a plot of the electric-field magnitude for the system described above with $I = 1.5 \times 10^{15}$ W/cm^2 at 4 ps, which is sufficiently long compared to the CBET saturation time [56] that a steady-state condition is achieved. The red arrows in Fig. 2(a) indicate the directions of the laser beams, which are injected as plane waves with 20-μm-wide, sixth-order, super-Gaussian envelopes. The beams are also s-polarized with their electric field vectors pointing out of the plane. Such an alignment of polarities represents a "worst case" scenario for analyzing CBET in a two-dimensional simulation since the ponderomotive force created by two such overlapping beams is a maximum. In the example in Fig. 2(a), approximately 79% of the downwardly directed laser power is steadily transferred to the diagonal beam.

A plot of the corresponding value of $|\delta n / n_0|$ at 4 ps appears in Fig. 2(b). This figure also indicates the direction of $\mathbf{k}_1$
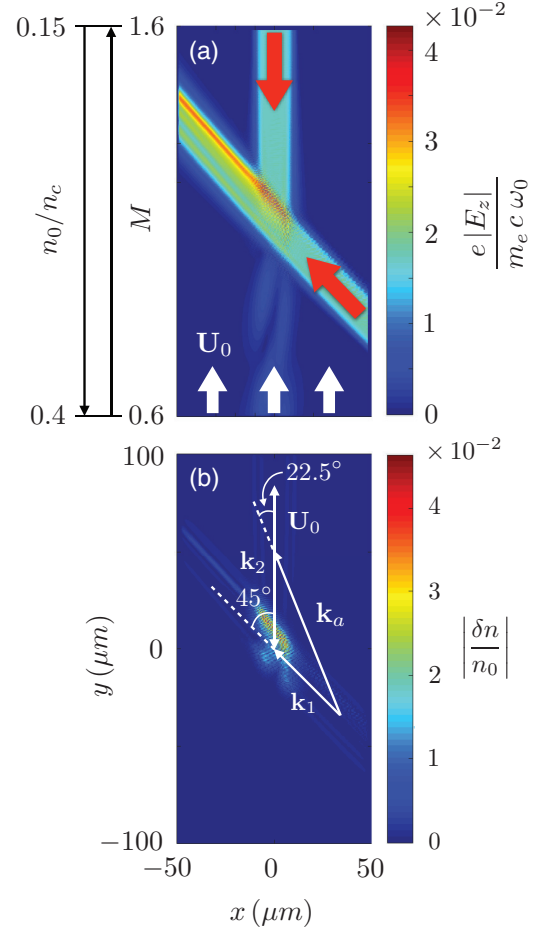

FIG. 2. Results from LPSE showing (a) the electric-field magnitude and (b) the absolute value of the electron-number-density perturbation at 4 ps. In this simulation, two laser beams (red arrows) with equal intensity $I = 1.5 \times 10^{15}$ W/cm^2 cross at $45°$ in an expanding, supersonic CH plasma with $T_e = 3$ keV and $T_i = 1$ keV. Resonance occurs near the crossing point where $M \simeq 1.1$ and $|\delta n / n_0| \lesssim 4\%$. Approximately 79% of the laser power is transferred, as indicated by the yellow and red regions of the diagonal beam in (a).

and $\mathbf{k}_2$ for the lasers, as well as the wave vector $\mathbf{k}_a$ of the interference pattern they create, which intersects $\mathbf{U}_0$ at an angle $\theta = 22.5°$. Note that $k_a = 2k \sin (\pi/2 - \theta)$, where $k = k_1 = k_2 = (2\pi/\lambda_0)(1 - n_e/n_c)^{1/2}$ and $\lambda_0 = 351$ nm is the vacuum laser wavelength. Because the lasers have equal frequencies ($\omega_1 = \omega_2$), resonance occurs in the plasma region where the Mach number satisfies $M = 1/\cos \theta \simeq 1.1$. Consequently, in order to maximize the CBET effect, our simulations were arranged to have this value of M near the center of the computational domain where the lasers cross. We also note that because $\omega_1 = \omega_2$, the electron-number-density perturbation δn is static in the laboratory frame and reaches a maximum of only about $0.04 \, n_0$, thus corroborating the linear approximations made in Eqs. (3) and (4).

Let us next consider the effect of finite laser bandwidth on CBET for this plasma configuration. To model bandwidth, we divide each laser into 20 monochromatic beamlets whose wavelengths are distributed symmetrically about λ_0 and whose intensities follow a Gaussian distribution (see inset of Fig. 3).
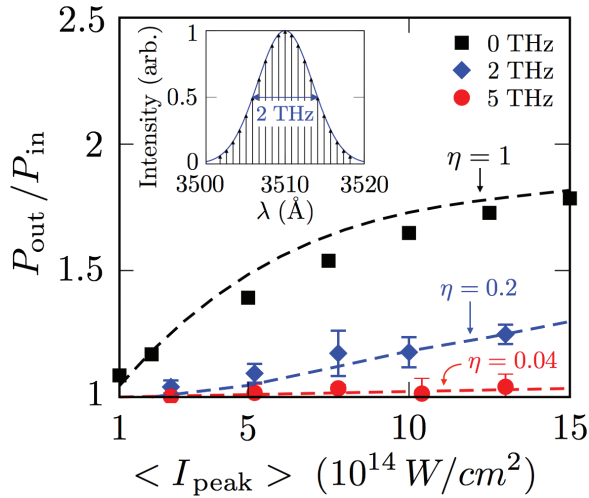
FIG. 3. Plots of the laser-power amplification due to CBET as a function of average peak intensity and bandwidth for the laser and plasma configuration shown in Fig. 2. The symbols denote results from wave-based LPSE simulations, while the dashed lines are predictions based on the steady-state theory described in the text. The inset shows the discrete multiline model of laser bandwidth used in this study for the case $\Delta \nu = 2$ THz.

Such a spectrum qualitatively resembles the bandwidth produced by SRRS. In our simulations, a uniform line spacing of 0.8 Å was used for $\Delta \nu = 2$ THz, while 2 Å was used for $\Delta \nu = 5$ THz—both of which are sufficiently small to expect equivalence with a continuous spectrum [40]. The different wavelengths for each bandwidth were randomly phased and eight runs were performed at each intensity to compute an ensemble average of the amplification of laser power in the enhanced beam, $P_{\text{out}}/P_{\text{in}}$. This quantity was computed by integrating the Poynting flux over the cross section of the intensified beam before and after passage through the CBET region and taking the ratio. The symbols in Fig. 3 are LPSE simulation results that show the dependence of $P_{\text{out}}/P_{\text{in}}$ on the peak laser intensity averaged over an interval of 20 ps, where error bars denote the standard deviation of the average result. Note that in the absence of CBET, $P_{\text{out}}/P_{\text{in}} = 1$.

Inspection of Fig. 3 shows that for $\Delta \nu = 0$ THz, the CBET process is responsible for a laser-power transfer of about 65% at $I = 10^{15}$ W/cm^2. For $\Delta \nu = 2$ THz, however, the transferred power drops significantly. At 5 THz, nearly complete suppression of CBET occurs. The observed mitigation is apparently due to the laser coherence time $\tau_c \simeq \Delta \nu^{-1}$ being much shorter than the time required for CBET to reach steady state ($\gtrsim 1$ ps) [45]. Thus, the interference pattern created by the beating of the lasers becomes out of phase with the ion-acoustic wave *before* the latter can reach a large amplitude. (This conclusion is supported by the fact that increasing ν_a by 50% or more did not affect our finite-bandwidth results.) Additionally, we note that the interaction length in these simulations ($\simeq 28$ μm) was too short for the laser coherence length ($\gtrsim 60$ μm) to be a factor.

To compare our results with theory, we adopt the steady-state, convective-growth model of CBET scattering developed in Ref. [10]. According to the theory, the amplification or

attenuation in intensity of an *s*-polarized light ray along a path ℓ is the exponential of the gain

$$G = \int \eta L_{\text{CBET}}^{-1} d\ell, \tag{5}$$

where η is a dimensionless parameter satisfying $0 \leqslant \eta \leqslant 1$ that has been included in the model to account for the effects of bandwidth and $L_{\text{CBET}}^{-1} \simeq 0.06 \lambda_{\mu m} I_{14}(n_e/n_c) R(\varphi)/[(T_e + 3T_i/Z)(1 - n_e/n_c)^{1/2}]$ is the inverse scale length of gain due to CBET (in units of μm^{-1}). Here, $\lambda_{\mu m}$ is the vacuum laser wavelength in microns, I_{14} is the crossing-laser intensity in units of 10^{14} W/cm^2, T_e and T_i are measured in keV and $R(\varphi) = (\nu_a/k_a c_s) \varphi/[(\nu_a/k_a c_s)^2 \varphi^2 + (1 - \varphi^2)^2]$, where $\varphi = \mathbf{k}_a \cdot \mathbf{U}/k_a c_s - (\omega_1 - \omega_2)/k_a c_s$, determines how closely the resonance condition in Eq. (1) is satisfied.

The theoretical model described above was used to estimate the power of the CBET-amplified beam in Fig. 2(a) over a range of laser intensities. This was accomplished by numerically computing Eq. (5) along many laser ray trajectories using the local plasma conditions and accounting for all possible crossing points of the monochromatic rays in the two-dimensional domain [57]. Such an approach is similar to the technique used to calculate CBET effects in ICF hydrocodes [18,58], with the exception that corrections due to inverse bremsstrahlung and temporal variations in the background density profile were not included in our calculations. The net Poynting flux resulting from this procedure with $\eta = 1$ was then integrated across the beam cross section to determine $P_{\text{out}}/P_{\text{in}}$, which is shown as the black curve in Fig. 3. Although the theory exceeds the (monochromatic) simulation result over most of the intensity range, the agreement is reasonably good considering the limitations of the former, which include a reliance on the paraxial approximation and the neglect of diffraction effects. Figure 3 also shows the laser-power amplification based on the monochromatic theory and the values $\eta = 0.2$ and $\eta = 0.04$—choices that reproduce the simulation results for $\Delta \nu = 2$ and 5 THz, respectively, fairly well. A heuristic expression that appears to capture the dependence of η on bandwidth in this study is the Lorentzian function $\eta \simeq 1/[1 + (\Delta \omega/\pi \nu_a)^2]$, which we note is similar in form to the result derived for a single discrete separation of laser frequencies [9,59].

In summary, we have identified a promising mechanism for the mitigation of CBET in directly driven ICF targets, namely, enhanced laser bandwidth. Although it has been suspected for some time that large bandwidths are helpful at controlling other categories of laser-plasma instabilities by detuning the underlying resonant interactions [26–31], a numerical demonstration of the efficacy of this approach for suppressing CBET has, to our knowledge, not been presented previously. Our results, which were obtained with the code LPSE [42,43], utilized a collection of randomly phased narrow-band lines to model laser bandwidth and showed that a significant reduction in CBET occurs for bandwidths of $2-5$ THz (corresponding to $\Delta \omega/\omega_0 \simeq 0.2\%-0.6\%$, respectively, at $\lambda_0 = 351$ nm) under conditions relevant to inhomogeneous, direct-drive ICF plasmas. Future computational research efforts with LPSE will explore the effects that laser speckles [60] and beam-smoothing techniques such as SSD [61,62] and ISI [63–66] have on CBET, as well as other single-beam and multibeam laser-plasma instabilities.

Although multiterahertz bandwidths exceed those of most ICF lasers in existence today, it may be possible to enhance the spectrum of narrow-band laser light to such levels by exploiting the phenomenon of SRRS in a diatomic gas medium [44,45]. Bandwidths up to 8 THz have been achieved on a frequency-doubled Nd:glass laser ($\lambda_0 = 527$ nm) using this technique in nitrogen gas [40]. Alternatively, the required bandwidth for CBET mitigation could likely be obtained directly by imploding ICF targets with *excimer* lasers. On the Nike KrF laser, for example, a full-width-half-maximum bandwidth of about 2.7 THz ($\tau_c \simeq 0.35$ ps) at full energy was achieved by employing etalons to shape the input power spectrum [67]. An argon-fluoride (ArF) laser has a larger native bandwidth than its KrF counterpart [68] and we project that at least 5 THz bandwidth could be similarly obtained in a high-energy ArF system [69]. Both KrF and ArF lasers have the additional advantage of possessing a short wavelength — 248 and 193 nm, respectively — which would help to suppress CBET even further.

[1] S. Atzeni and J. Meyer-ter-Vehn, *The Physics of Inertial Fusion* (Clarendon Press, Oxford, 2004).

[2] W. L. Kruer, *The Physics of Laser Plasma Interactions* (Westview Press, Boulder, 2003).

[3] P. Michel, L. Divol, E. A. Williams, S. Weber, C. A. Thomas, D. A. Callahan, S. W. Haan, J. D. Salmonson, S. Dixit, D. E. Hinkel, M. J. Edwards, B. J. MacGowan, J. D. Lindl, S. H. Glenzer, and L. J. Suter, Phys. Rev. Lett. **102**, 025004 (2009).

[4] P. Michel, S. H. Glenzer, L. Divol, D. K. Bradley, D. Callahan, S. Dixit, S. Glenn, D. Hinkel, R. K. Kirkwood, J. L. Kline, W. L. Kruer, G. A. Kyrala, S. Le Pape, N. B. Meezan, R. Town, K. Widmann, E. A. Williams, B. J. MacGowan, J. Lindl, and L. J. Suter, Phys. Plasmas **17**, 056305 (2010).

[5] S. H. Glenzer, B. J. MacGowan, P. Michel, N. B. Meezan, L. J. Suter, S. N. Dixit, J. L. Kline, G. A. Kyrala, D. K. Bradley, D. A. Callahan, E. L. Dewald, L. Divol, E. Dzenitis, M. J. Edwards, A. V. Hamza, C. A. Haynam, D. E. Hinkel, D. H. Kalantar, J. D. Kilkenny, O. L. Landen, J. D. Lindl, S. LePape, J. D. Moody, A. Nikroo, T. Parham, M. B. Schneider, R. P. Town, P. Wegner, K. Widmann, P. Whitman, B. K. Young, B. Van Wonterghem, L. J. Atherton, and E. I. Moses, Science **327**, 1228 (2010).

[6] N. B. Meezan, L. J. Atherton, D. A. Callahan, E. L. Dewald, S. Dixit, E. G. Dzenitis, M. J. Edwards, C. A. Haynam, D. E. Hinkel, O. S. Jones, O. Landen, R. A. London, P. A. Michel, J. D. Moody, J. L. Milovich, M. B. Schneider, C. A. Thomas, R. P. J. Town, A. L. Warrick, S. V. Weber, K. Widmann, S. H. Glenzer, L. J. Suter, B. J. MacGowan, J. L. Kline, G. A. Kyrala, and A. Nikroo, Phys. Plasmas **17**, 056304 (2010).

[7] R. P. J. Town, M. D. Rosen, P. A. Michel, L. Divol, J. D. Moody, G. A. Kyrala, M. B. Schneider, J. L. Kline, C. A. Thomas, J. L. Milovich, D. A. Callahan, N. B. Meezan, D. E. Hinkel, E. A. Williams, R. L. Berger, M. J. Edwards, L. J. Suter, S. W. Haan, J. D. Lindl, E. L. Dewald, S. Dixit, S. H. Glenzer, O. L. Landen, E. I. Moses, H. A. Scott, J. A. Harte, and G. B. Zimmerman, Phys. Plasmas **18**, 056302 (2011).

[8] G. A. Kyrala, J. L. Kline, S. Dixit, S. Glenzer, D. Kalantar, D. Bradley, N. Izumi, N. Meezan, O. Landen, D. Callahan, S. V. Weber, J. P. Holder, S. Glenn, M. J. Edwards, J. Koch, L. J. Suter, S. W. Haan, R. P. J. Town, P. Michel, O. Jones, S. Langer, J. D. Moody, E. L. Dewald, T. Ma, J. Ralph, A. Hamza, E. Dzenitis, and J. Kilkenny, Phys. Plasmas **18**, 056307 (2011).

[9] W. L. Kruer, S. C. Wilks, B. B. Afeyan, and R. K. Kirkwood, Phys. Plasmas **3**, 382 (1996).

[10] C. J. Randall, J. R. Albritton, and J. J. Thomson, Phys. Fluids **24**, 1474 (1981).

[11] R. W. Short and E. A. Williams, Phys. Rev. Lett. **47**, 337 (1981).

[12] V. V. Eliseev, W. Rozmus, V. T. Tikhonchuk, and C. E. Capjack, Phys. Plasmas **3**, 2215 (1996).

[13] C. J. McKinstrie, J. S. Li, R. E. Giacone, and H. X. Vu, Phys. Plasmas **3**, 2686 (1996).

[14] H. A. Rose and S. Ghosal, Phys. Plasmas **5**, 1461 (1998).

[15] B. I. Cohen, B. F. Lasinski, A. B. Langdon, E. A. Williams, K. B. Wharton, R. K. Kirkwood, and K. G. Estabrook, Phys. Plasmas **5**, 3408 (1998).

[16] E. A. Williams, B. I. Cohen, L. Divol, M. R. Dorr, J. A. Hittinger, D. E. Hinkel, A. B. Langdon, R. K. Kirkwood, D. H. Froula, and S. H. Glenzer, Phys. Plasmas **11**, 231 (2004).

[17] J. A. F. Hittinger, M. R. Dorr, R. L. Berger, and E. A. Williams, J. Comput. Phys. **209**, 695 (2005).

[18] I. V. Igumenshchev, D. H. Edgell, V. N. Goncharov, J. A. Delettrez, A. V. Maximov, J. F. Myatt, W. Seka, A. Shvydky, S. Skupsky, and C. Stoeckl, Phys. Plasmas **17**, 122708 (2010).

[19] A. K. Davis, D. Cao, D. T. Michel, M. Hohenberger, D. H. Edgell, R. Epstein, V. N. Goncharov, S. X. Hu, I. V. Igumenshchev, J. A. Marozas, A. V. Maximov, J. F. Myatt, P. B. Radha, S. P. Regan, T. C. Sangster, and D. H. Froula, Phys. Plasmas **23**, 056306 (2016).

[20] I. V. Igumenshchev, W. Seka, D. H. Edgell, D. T. Michel, D. H. Froula, V. N. Goncharov, R. S. Craxton, L. Divol, R. Epstein, R. Follett, J. H. Kelly, T. Z. Kosc, A. V. Maximov, R. L. McCrory, D. D. Meyerhofer, P. Michel, J. F. Myatt, T. C. Sangster, A. Shvydky, S. Skupsky, and C. Stoeckl, Phys. Plasmas **19**, 056314 (2012).

[21] T. R. Boehly, D. L. Brown, R. S. Craxton, R. L. Keck, J. P. Knauer, J. H. Kelly, T. J. Kessler, S. A. Kumpan, S. J. Loucks, S. A. Letzring, F. J. Marshall, R. L. McCrory, S. F. B. Morse, W. Seka, J. M. Soures, and C. P. Verdon, Opt. Commun. **133**, 495 (1997).

[22] V. N. Goncharov, T. C. Sangster, R. Betti, T. R. Boehly, M. J. Bonino, T. J. B. Collins, R. S. Craxton, J. A. Delettrez, D. H. Edgell, R. Epstein, R. K. Follett, C. J. Forrest, D. H. Froula, V. Yu. Glebov, D. R. Harding, R. J. Henchen, S. X. Hu, I. V. Igumenshchev, R. Janezic, J. H. Kelly, T. J. Kessler, T. Z. Kosc, S. J. Loucks, J. A. Marozas, F. J. Marshall, A. V. Maximov, R.

L. McCrory, P. W. McKenty, D. D. Meyerhofer, D. T. Michel, J. F. Myatt, R. Nora, P. B. Radha, S. P. Regan, W. Seka, W. T. Shmayda, R. W. Short, A. Shvydky, S. Skupsky, C. Stoeckl, B. Yaakobi, J. A. Frenje, M. Gatu-Johnson, R. D. Petrasso, and D. T. Casey, Phys. Plasmas **21**, 056315 (2014).

[23] J. A. Marozas, M. Hohenberger, M. J. Rosenberg, D. Turnbull, T. J. B. Collins, P. B. Radha, P. W. McKenty, J. D. Zuegel, F. J. Marshall, S. P. Regan, T. C. Sangster, W. Seka, E. M. Campbell, V. N. Goncharov, M. W. Bowers, J.-M. G. Di Nicola, G. Erbert, B. J. MacGowan, L. J. Pelz, and S. T. Yang, Phys. Rev. Lett. **120**, 085001 (2018).

[24] D. H. Froula, T. J. Kessler, I. V. Igumenshchev, R. Betti, V. N. Goncharov, H. Huang, S. X. Hu, E. Hill, J. H. Kelly, D. D. Meyerhofer, A. Shvydky, and J. D. Zuegel, Phys. Plasmas **20**, 082704 (2013).

[25] D. M. Kehne, M. Karasik, Y. Aglitsky, Z. Smyth, S. Terrell, J. L. Weaver, Y. Chan, R. H. Lehmberg, and S. P. Obenschain, Rev. Sci. Instrum. **84**, 013509 (2013).

[26] G. M. Zablavskii and V. S. Zakharov, Sov. Phys. Tech. Phys. **12**, 7 (1967).

[27] E. J. Valeo and C. R. Oberman, Phys. Rev. Lett. **30**, 1035 (1973).

[28] J. J. Thompson and J. I. Karush, Phys. Fluids **17**, 1608 (1974).

[29] J. J. Thompson, Nucl. Fusion **15**, 237 (1975).

[30] G. Laval, R. Pellat, D. Pesme, A. Ramani, M. N. Rosenbluth, and E. A. Williams, Phys. Fluids **20**, 2049 (1977).

[31] S. P. Obenschain, N. C. Luhmann, Jr., and P. T. Greiling, Phys. Rev. Lett. **36**, 1309 (1976).

[32] K. Estabrook, J. Harte, E. M. Campbell, F. Ze, D. W. Phillion, M. D. Rosen, and J. T. Larsen, Phys. Rev. Lett. **46**, 724 (1981).

[33] S. P. Obenschain and N. C. Luhmann, Jr., Appl. Phys. Lett. **30**, 452 (1977).

[34] H. A. Baldis, E. M. Campbell, and W. L. Kruer, in *Handbook of Plasma Physics*, edited by M. N. Rosenbluth and R. Z. Sagdeev, Physics of Laser Plasma Vol. 3, edited by A. M. Rubenchik and S. Witkowski (Elsevier, Amsterdam, 1991), Chap. 9.

[35] W. L. Kruer, Phys. Fluids B **3**, 2356 (1991).

[36] D. Eimerl, W. L. Kruer, and E. M. Campbell, Comments Plasma Phys. Controlled Fusion **15**, 85 (1992).

[37] G. Bonnaud and C. Reisse, Nucl. Fusion **26**, 633 (1986).

[38] H. Yoneda, T. Miura, Y. Yokota, Y. Motoki, A. Sasaki, K. Ueda, and H. Takuma, Laser Part. Beams **11**, 15 (1993).

[39] Y. Zhao, S. Weng, M. Chen, J. Zheng, H. Zhuo, and Z. Sheng, Matter Radiat. Extremes **2**, 190 (2017).

[40] D. Eimerl, D. Milam, and J. Yu, Phys. Rev. Lett. **70**, 2738 (1993).

[41] Bandwidths on OMEGA and NIF are currently about 1 and 0.3 THz, respectively, due to limitations associated with the efficient frequency conversion of Nd:glass laser light.

[42] J. F. Myatt, R. K. Follett, J. G. Shaw, D. H. Edgell, D. H. Froula, I. V. Igumenshchev, and V. N. Goncharov, Phys. Plasmas **24**, 056308 (2017).

[43] J. F. Myatt, J. G. Shaw, R. K. Follett, D. H. Edgell, and D. H. Froula, J. Comput. Phys. (to be published).

[44] N. Bloembergen, *Nonlinear Optics*, 4th ed. (World Scientific, Singapore, 1996).

[45] W. Kaiser and M. Maier, in *Laser Handbook*, edited by F. T. Arecchi and E. O. Schulz-Dubois (North Holland, Amsterdam, 1972).

[46] J. Weaver, R. Lehmberg, S. Obenschain, D. Kehne, and M. Wolford, Appl. Opt. **56**, 1 (2017).

[47] R. L. Berger, C. H. Still, E. A. Williams, and A. B. Langdon, Phys. Plasmas **5**, 4337 (1998).

[48] C. H. Still, R. L. Berger, A. B. Langdon, D. E. Hinkel, L. J. Suter, and E. A. Williams, Phys. Plasmas **7**, 2023 (2000).

[49] G. Riazuelo and G. Bonnaud, Phys. Plasmas **7**, 3841 (2000).

[50] A. Taflove and S. C. Hagness, *Computational Electrodynamics: The Finite-Difference Time-Domain Method*, 3rd. ed. (Artech House, Boston, 2005).

[51] D. M. Sullivan, *Electromagnetic Simulation Using FDTD Method*, 2nd ed. (Wiley, New Jersey, 2004).

[52] D. E. Merewether, R. Fisher, and F. W. Smith, IEEE Trans. Nucl. Sci. **27**, 1829 (1980).

[53] X. Antoine, A. Arnold, C. Besse, M. Ehrhardt, and A. Schädle, Commun. Comput. Phys. **4**, 729 (2008).

[54] H. A. Rose, Phys. Plasmas **3**, 1709 (1996).

[55] E. A. Williams, R. L. Berger, R. P. Drake, A. M. Rubenchik, B. S. Bauer, D. D. Meyerhofer, A. C. Gaeris, and T. W. Johnston, Phys. Plasmas **2**, 129 (1995).

[56] The time required for monochromatic CBET saturation in this study is approximately the laser transit time across the computational domain, $\simeq 0.7$ ps, plus the ion-wave damping time, $v_a^{-1} \simeq 0.5$ ps, or about 1.2 ps in total.

[57] R. K. Follett, D. H. Edgell, D. H. Froula, V. N. Goncharov, I. V. Igumenshchev, J. G. Shaw, and J. F. Myatt, Phys. Plasmas **24**, 103128 (2017).

[58] D. H. Edgell, R. K. Follett, I. V. Igumenshchev, J. F. Myatt, J. G. Shaw, and D. H. Froula, Phys. Plasmas **24**, 062706 (2017).

[59] R. K. Kirkwood, B. B. Afeyan, W. L. Kruer, B. J. MacGowan, J. D. Moody, D. S. Montgomery, D. M. Pennington, T. L. Weiland, and S. C. Wilks, Phys. Rev. Lett. **76**, 2065 (1996).

[60] G. Raj and S. Hüller, Phys. Rev. Lett. **118**, 055002 (2017).

[61] S. Skupsky, R. W. Short, T. Kessler, R. S. Craxton, S. Letzring, and J. M. Soures, J. Appl. Phys. **66**, 3456 (1989).

[62] S. P. Regan, J. A. Marozas, J. H. Kelly, T. R. Boehly, W. R. Donaldson, P. A. Jaanimagi, R. L. Keck, T. J. Kessler, D. D. Meyerhofer, W. Seka, S. Skupsky, and V. A. Smalyuk, J. Opt. Soc. Am. B **17**, 1483 (2000).

[63] R. H. Lehmberg and S. P. Obenschain, Opt. Commun. **46**, 27 (1983).

[64] S. P. Obenschain, J. Grun, M. J. Herbst, K. J. Kearney, C. K. Manka, E. A. McLean, A. N. Mostovych, J. A. Stamper, R. R. Whitlock, S. E. Bodner, J. H. Gardner, and R. H. Lehmberg, Phys. Rev. Lett. **56**, 2807 (1986).

[65] S. P. Obenschain, R. H. Lehmberg, D. Kehne, F. Hegeler, M. Wolford, J. Sethian, J. Weaver, and M. Karasik, Appl. Opt. **54**, 103 (2015).

[66] A. N. Mostovych, S. P. Obenschain, J. H. Gardner, J. Grun, K. J. Kearney, C. K. Manka, E. A. McLean, and C. J. Pawley, Phys. Rev. Lett. **59**, 1193 (1987).

[67] S. P. Obenschain, S. E. Bodner, D. Colombant, K. Gerber, R. H. Lehmberg, E. A. McLean, A. N. Mostovych, M. S. Pronko, C. J. Pawley, A. J. Schmitt, J. D. Sethian, V. Serlin, J. A. Stamper, and C. A. Sullivan, Phys. Plasmas **3**, 2098 (1996).

[68] H. F. Döbele, M. Hörl, and M. Röwekamp, Appl. Phys. B **42**, 67 (1987).

[69] M. W. McGeoch (private communication).